

# *In vivo* documentation of cutaneous inflammation using spectral imaging

Georgios N. Stamatias  
Nikiforos Kollias

Johnson & Johnson Consumer Products Company  
Division of Johnson & Johnson Consumer  
Companies, Inc.  
Methods and Models Development  
Skillman, New Jersey 08558

**Abstract.** Typical manifestations of cutaneous inflammation include erythema and edema. While erythema is the result of capillary dilation and local increase of oxygenated hemoglobin concentration, edema is characterized by an increase in extracellular fluid in the dermis, leading to local tissue swelling. Both of these inflammatory reactions are typically graded visually. We demonstrate the potential of spectral imaging as an objective noninvasive method for quantitative documentation of both erythema and edema. As examples of dermatological conditions that exhibit skin inflammation we applied this method on patients suffering from (1) allergic dermatitis (poison ivy rashes), (2) inflammatory acne, and (3) viral infection (herpes zoster). Spectral images are acquired in the visible and near-IR part of the spectrum. Based on a spectral decomposition algorithm, apparent concentrations maps are constructed for oxyhemoglobin, deoxyhemoglobin, melanin, optical scattering, and water. In each dermatological condition examined, the concentration maps of oxyhemoglobin and water represent quantitative visualizations of the intensity and extent of erythema and cutaneous edema, correspondingly. We demonstrate that spectral imaging can be used to quantitatively document parameters relevant to skin inflammation. Applications may include monitoring of disease progression as well as screening for efficacy of treatments. © 2007 Society of Photo-Optical Instrumentation Engineers. [DOI: 10.1117/1.2798704]

Keywords: spectral imaging; erythema; poison ivy; dermatitis; herpes zoster; acne.

Paper 07141SSR received Apr. 16, 2007; revised manuscript received Jul. 4, 2007; accepted for publication Jul. 17, 2007; published online Oct. 19, 2007.

## 1 Introduction

An inflammatory skin reaction is accompanied by redness (erythema, rubor) of the involved skin area and often with localized tissue swelling (edema, tumor).

In the early phase of acute tissue inflammation, mediators such as histamine, bradykinin, and various prostaglandins relax the smooth muscle layer of arteries and arterioles. The resulting vasodilation leads to increased blood volume in the inflamed area that is clinically perceived as visible erythema. Both oxyhemoglobin (oxy-Hb) and deoxyhemoglobin (deoxy-Hb) in blood absorb strongly in the blue and green parts of the visible spectrum but very weakly in the red part. Therefore light that is remitted from an inflamed skin site appears to be red compared to the surrounding uninvolved skin.

Inflammatory mediators such as histamine, bradykinin, and leukotrienes may also act to increase the permeability of the vascular walls to blood plasma, which could result in increased concentration of extracellular fluid in the tissue. Under physiological conditions, lymphatic vessels drain the excess fluid,<sup>1</sup> but their draining capacity can be exceeded during

an inflammatory reaction, which leads to local accumulation of extracellular fluid (exudate).

Cutaneous edema and erythema are typically evaluated clinically using a visual analogue scale. Being subjective, this method depends on the experience of the clinician. Accurate objective documentation through imaging is often required to monitor the evolution of the cutaneous inflammation.

Taking advantage of the particular spectroscopic properties in the visible part of the spectrum of oxy-Hb and deoxy-Hb, their apparent concentrations in the skin can be evaluated by spectroscopic analysis of the light remitted from the skin, a method known as diffuse reflectance spectroscopy<sup>2-8</sup> (DRS). It has been shown<sup>5</sup> that erythema directly relates to increased apparent concentrations of oxy-Hb, while accumulation of deoxy-Hb relates to blood stasis.<sup>9</sup> Recent advances in digital imaging hardware (optics, detectors, frame-grabbers, etc.) have enabled the development of spectral imaging, which in addition to the spectral information similar to that obtained by DRS, provides 2-D spatial information.<sup>10-13</sup> More precisely, it provides the means to localize and quantify cutaneous erythema.<sup>14,15</sup>

In the case of edema the excess fluid is composed primarily of water. The light absorption properties of water in the near IR (NIR) can be used to estimate the severity of the

Address all correspondence to Georgios Stamatias, Johnson & Johnson, 199 Grandview Rd, Skillman, NJ 08558; Tel: (908)874-2542; Fax:(908) 874-7205; E-mail: gstamat@cpcus.jnj.com

edema reaction.<sup>16,17</sup> Similar to the case of erythema, spectral imaging provides the means to localize and quantify the cutaneous edema reaction.<sup>15</sup>

In this paper, we present the potential of spectral imaging as a noninvasive method for quantitative documentation of skin inflammation. We present several examples of diverse dermatological conditions including inflammatory acne, herpes zoster, and rhus dermatitis (poison ivy rashes).

## 2 Materials and Methods

### 2.1 Clinical Protocols

All clinical investigations were conducted according to the declaration of Helsinki principles. In the first study, five healthy individuals (male and female, 18 to 60 years of age, fair complexioned, skin types II to IV) without an active skin disease including eczema, urticaria, and history of atopic dermatitis and with positive history to rhus dermatitis volunteered to participate after giving informed consent. Rhus dermatitis was induced with an oleoresin extract.<sup>18</sup> The oleoresin urushiol is the cause for the allergic reaction when sensitized individuals come in contact with the poison ivy plant and its relatives. Briefly, 10  $\mu$ l of 1:50 dilution of poison oak/poison ivy urushiol were applied with disposable micropipettes to 0.6-cm-diam disks of filter paper. The disks were left open to the air for 30 min and carefully applied with forceps to each test site. The loaded filter paper disks were then covered with occlusive tape (3M Blenderm, St. Paul, Minnesota) and left in place for 2 h. After the designated time duration, the disks and tape were removed, and the sites were washed with liquid soap and water. Before each evaluation the volunteers were left for 20 min to equilibrate to ambient conditions of the test facility. Clinical evaluation by a dermatologist and spectral imaging were performed on days 1, 3, and 7 after initiation of the inflammation. The clinical evaluation was based on a five-grade scale.

In the second study, five healthy individuals (male and female, 18 to 40 years of age, fair complexioned, skin types II to IV) with mild inflammatory acne participated after giving informed consent. The qualified volunteers had a history of experiencing at least two new inflammatory lesions per week (data obtained through self-report). No treatment usage or change in existing skincare regimens was allowed for the duration of the study. The lesions were examined at baseline and at days 1, 2, 3, 4, and 7.

Finally, a patient (male, 63 years, Fitzpatrick skin type II) with inflammatory skin lesions in the jaw and neck area diagnosed with herpes zoster by a trained dermatologist gave his informed consent to be imaged with spectral imaging.

### 2.2 Instrumentation

We used a custom-made spectral imaging camera (MuSIS-HS, FORTH-Photonics, Athens, Greece) with 18 narrow-band filters (full width at half maximum of 10 nm) in the wavelength range of 400 to 970 nm and three broadband filters in the red, green, and blue spectral regions. The red, green, and blue filtered images were combined to compose a color image. The imaging detector was an 8-bit CCD camera with 1024  $\times$  768 pixels. The field of view was 16  $\times$  12 cm, resulting in a final image resolution of 0.156 mm/pixel for both the *x* and *y* axes. We used a filtered incandescent lamp

equipped with a linear polarizer (model v600, Syris Scientific, Gray, Maine) as the light source. To avoid specular reflections we placed a linear polarizer in front of the camera lens with its plane orthogonal to the plane of polarization of the illumination light. We acquired a series of spectral images at a variety of wavelengths in the visible and NIR spectral range. Acquisition took approximately 5 s per image (a series of a minimum of six images required for chromophore calculations took 30 s). Each series comprised a hyperspectral image stack, a 3-D cube with one spectral and two spatial dimensions. The images in the stack were aligned using a modified algorithm based on minimization of distance in the Fourier domain.<sup>19</sup> This step was enough to align the images within approximately 0.5 mm, at which level the skin tissue can be assumed to be homogeneous for the purposes of macroimaging. Each pixel in the hyperspectral image stack represented a remittance spectrum. Spectral images acquired using narrow-band filters contain information about the concentrations of chromophores that absorb light at the corresponding spectral bands and can therefore be qualitatively described based on absorption and scattering parameters. Note, however, that this information is not quantitative, partly due to the extensive overlap of the chromophore absorption profiles. To extract quantitative information about the concentrations of chromophores, the reflectance images must first be converted to optical density (absorbance) maps. Then spectral analysis algorithms can be applied on a pixel-by-pixel basis for the calculation of apparent concentrations of the chromophores. To this end, absorption spectra were calculated for each pixel as the negative logarithm of the ratio of image of interest to the image at 850 nm, where water, melanin, and hemoglobin absorptions are negligible. This normalization to the image at 850 nm also helps in minimizing artifacts due to contours. After these calculations, the resulting series of images constitutes the hyperspectral absorption image stack, where each pixel corresponds to an absorbance spectrum.

### 2.3 Erythema Maps

Erythema was evaluated based on the apparent concentrations of oxy-Hb. We calculated apparent concentrations of oxy-Hb and deoxy-Hb from the absorbance spectra after correction for melanin and scattering contributions according to a previously described algorithm.<sup>6,15,20,21</sup> We refer to the calculated concentrations as “apparent” because they are based on light absorption curves and they are given in relative units. They are expected to be linearly related to “absolute” concentrations of hemoglobins in units of mass per volume of tissue. Due to the inhomogeneous nature of the tissue, such absolute units do not represent the reality and may be confusing. Using the absorbance hyperspectral image stack described in the previous section we calculated oxy-Hb, deoxy-Hb, melanin, and scattering values by applying the already mentioned algorithm to the absorption spectrum corresponding to each pixel. Briefly, melanin and scattering contribution were calculated as the slope and the intercept of a straight line fitted in the 630 to 730-nm region. Then these contributions were subtracted from the original absorption spectra and the corrected spectra were fitted for the contributions of oxy-Hb and deoxy-Hb. Finally, we created distribution maps for each chromophore, in which the gray-scale intensity corresponded to the calcu-

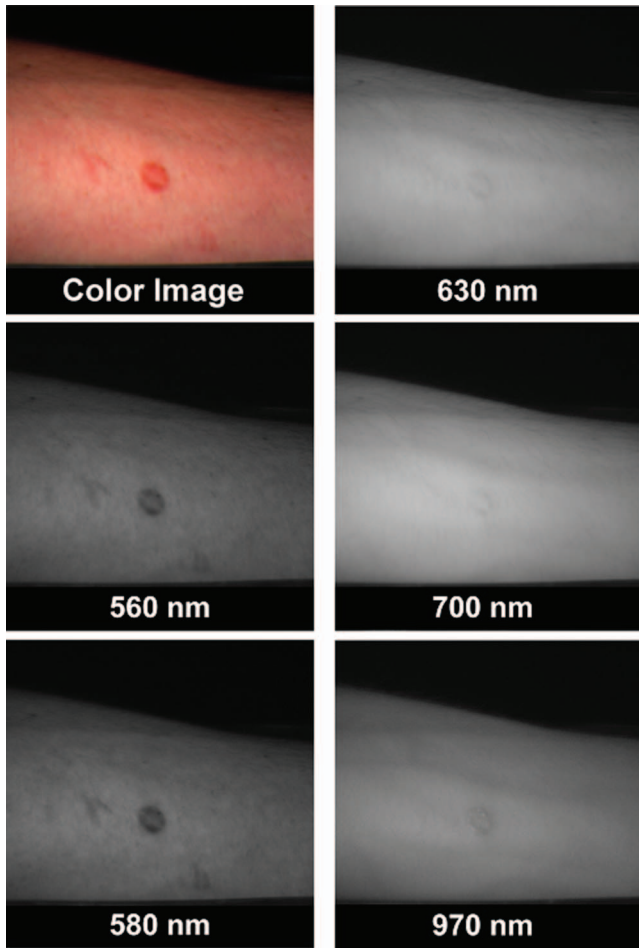


**Fig. 1** Images filtered at selected narrow bands demonstrate the optical properties of the tissue. An example of a color image and the corresponding series of narrow-band images acquired 1 week after initiation of rhus dermatitis. Hemoglobin absorption is maximum for the images at 560 and 580 nm. Deep vessels are evident at longer wavelengths. Water absorbs NIR radiation with a local maximum at 970 nm. The inflamed area looks dark at 970 nm due to edema.

lated chromophore values. Each chromophore map is a quantitative representation of the special distribution of the contribution to radiation absorption by the corresponding chromophore. Assuming that the contribution to light absorption is proportional to the chromophore concentration, the chromophore maps can be considered as quantitative representations of the chromophore concentrations. We considered the oxy-Hb map to represent a quantitative map of erythema involvement.<sup>5</sup> To quantitate erythema we used the average gray-scale value over a region of interest defined by the size of the lesion to be measured. A neighboring area of uninvolved skin of similar size was chosen for reference. The apparent concentration of oxy-Hb corresponding to neighboring uninvolved skin sites was subtracted.

#### 2.4 Edema Maps

NIR radiation is absorbed by water with a local maximum at 970 nm. Water absorbance maps were calculated as the negative logarithm of the pixel intensity values of the image at 970 nm, where water has an absorption maximum, normal-

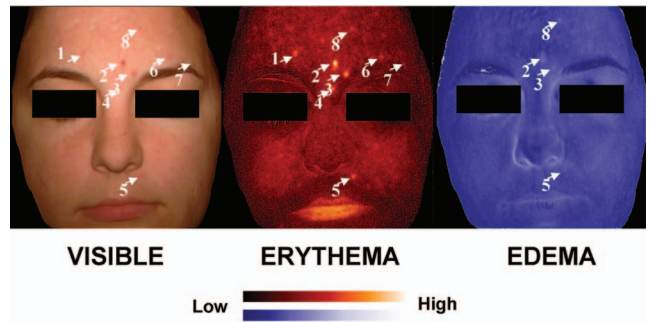


**Fig. 4** Erythema and edema maps can be used to extract parameters relevant to acne. Here, the visible image and the corresponding pseudocolored erythema and edema maps are shown. The color bar indicates the relative intensity for the erythema and edema. A lesion count can be performed easily on the oxy-Hb (erythema) map. The intensity and extent of erythema are also evident. Note the high values of oxy-Hb on the lips, indicating higher perfusion compared to surrounding skin. The intensity and extent of edema can be documented on the water distribution map. Not all lesions present edema.

ized to the corresponding pixel intensity values of the image at 850 nm (negligible NIR absorption by water). The normalization provides a baseline for the measurement of NIR absorption and minimizes artifacts due to contours. The amount of NIR absorption at 970 nm was assumed to be proportional to water content in the tissue. The absorbance map at 970 nm can be considered as a quantitative map of water accumulation in the tissue and therefore of edema. At these wavelength range light penetrates 1.2 to 1.6 mm into the skin,<sup>7</sup> and therefore the information about cutaneous edema is limited to the tissue volume corresponding to this depth. Similarly to erythema, apparent water concentration values were averaged

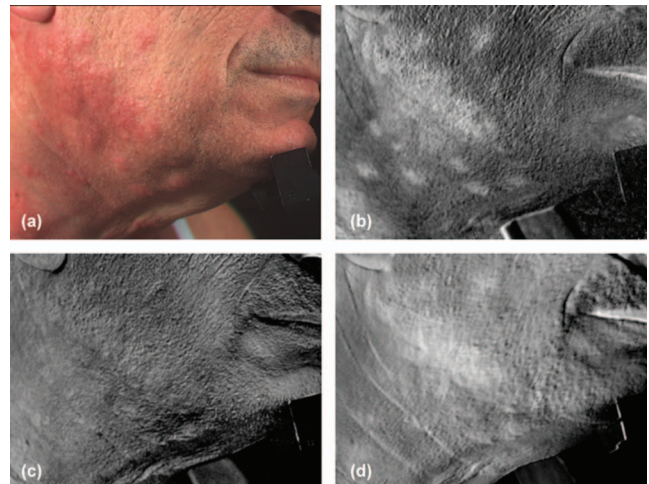


**Fig. 6** Documentation of cutaneous inflammation induced by a viral infection (herpes zoster). (a) Visible image, (b) oxy-Hb apparent concentration map relates to erythema, (c) deoxy-Hb apparent concentration map, and (d) water apparent concentration map relates to edema. In all the maps, the gray-scale depends linearly to the apparent concentration of the chromophore. The maximum gray-scale value (255) corresponds to apparent concentration of 10 for oxy-Hb, 10 for deoxy-Hb, and 0.5 for water. The minimum gray-scale intensity (0) corresponds to zero concentration for all the maps.

over a region of interest based on the lesion size. The apparent water concentration corresponding to neighboring uninvolved skin sites was subtracted.

### 3 Results

#### 3.1 Allergic Dermatitis (Poison Ivy)

The volar forearms of five volunteers with positive history to rhus dermatitis were induced by urushiol for 2 h under occlusion, and the reaction was followed for 1 week. On day 1 only, two subjects developed a mild rash, while on day 3 all of the volunteers had developed a reaction including erythema and edema. Erythema was intense and limited to the area where urushiol came in contact with the skin. Edema was mild and present as perifollicular swellings within the area of induction. On day 7, the reactions persisted on all volunteers and they appeared to be more uniform than on day 3.

An example of a series of spectral images, along with the corresponding color image, acquired 3 days after initiation of Rhus dermatitis are shown in Fig. 1. Hemoglobin absorption is maximum for the images at 560 and 580 nm and appears as dark areas in the corresponding images. At this wavelength range, light penetration is limited to a few hundred micrometers,<sup>4,7</sup> indicating that the observable features are limited to the superficial capillaries. Deeper vessels are evident at longer wavelengths, where both hemoglobins and melanin do not absorb strongly and light can travel deeper in the tissue up to a few-millimeters without being significantly attenuated. Although, in the range between 630 and 850 nm, melanin and hemoglobin absorption is minimal, the high concentration of hemoglobin at the inflamed areas provides the contrast to give rise to gray shadows. Water absorbs with a maximum at 970 nm and provides the contrast (appears dark) in the corresponding image due to local edema. Although we can describe the absorptions at each wavelength qualitatively, calculation of the chromophore values through spectral analysis is required to arrive at quantitative results.

In the chromophore maps shown in Fig. 2, it is evident that the urushiol-induced inflammatory reaction manifested significantly elevated concentrations of oxy-Hb compared to surrounding skin. Deoxy-Hb concentration was elevated moderately. The increased water concentration relates to edema formation. As expected, the inflammation did not affect the local melanin concentration. In all the maps, the intensity scale is linear to the apparent concentration.

We can extract quantitative information from the concentration maps using image analysis. For example, we can calculate the average value for the apparent erythema and edema after baseline subtraction. The erythema values calculated from the oxy-Hb concentration maps in this way were in good agreement with clinical evaluation by the physician as demonstrated by the correlation coefficient  $R=0.979$  (data shown in Fig. 3).

#### 3.2 Acne

Spectral imaging was used to evaluate the intensity and extent of erythema and edema in acne lesions. The lesions were monitored over a period of 1 week. Similarly to the poison ivy study, erythema maps were constructed based on the oxy-Hb apparent concentration values calculated from the spectral images.

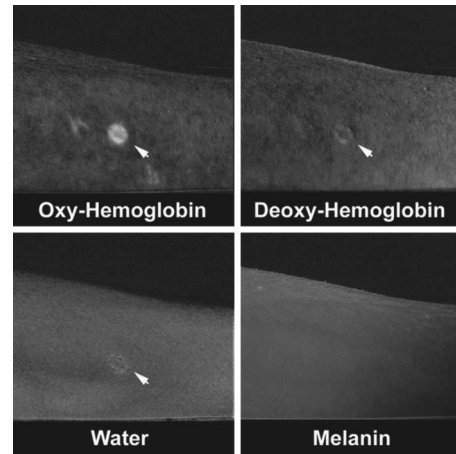


**Fig. 2** Apparent concentration maps for the skin chromophores demonstrate the intensity and spatial distribution of erythema and edema. The maps shown here were calculated from the images shown in Fig. 1. The urushiol-induced inflammatory reaction demonstrates significantly elevated concentration of oxy-Hb compared to surrounding skin. Deoxy-Hb concentration is elevated moderately and the increased water concentration relates to edema formation. For comparison, the melanin map is also shown. Inflammation has not affected the local melanin concentration. In all the maps the scale is linear. The maximum gray-scale value (255) corresponds to apparent concentration of 10 for oxy-Hb, deoxy-Hb, and melanin, and 0.5 for water. The minimum gray-scale intensity (0) corresponds to zero concentration for all the maps.

Based on spectral imaging of the whole face we created erythema and edema maps (Fig. 4). Lesion count, an important parameter in acne clinical trials, is easier to perform on the erythema image rather than the traditional way on the RGB image, due to the improved image contrast. Furthermore, this procedure can be automated using appropriate image-thresholding limits. It is interesting to note that in the erythema map, the lips appear to be brighter than the surrounding skin, indicating the high degree of vascularization of

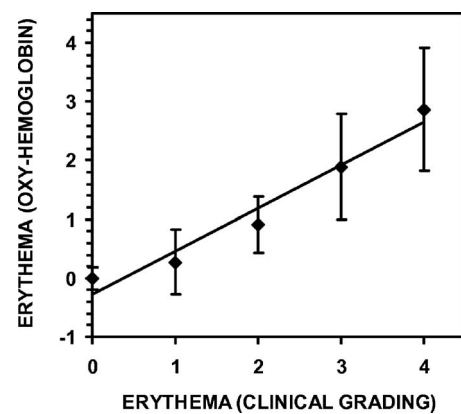
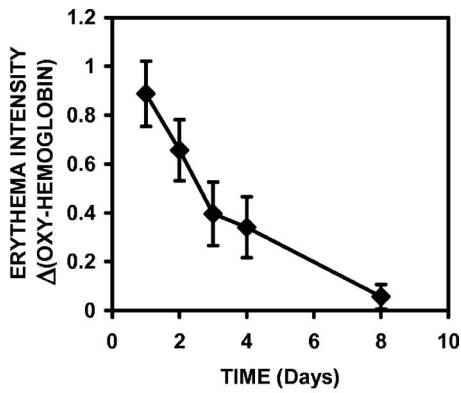
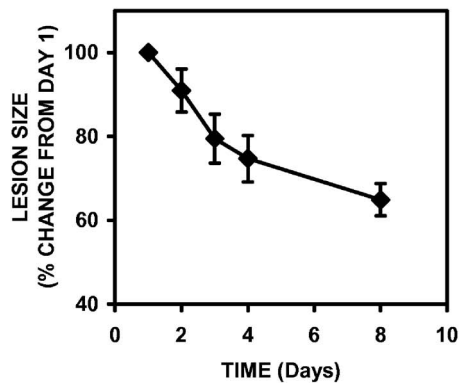


**Fig. 3** Erythema values obtained by spectral image analysis correlate with the clinical evaluation. Clinical evaluation of erythema was based on five-scale grading (0 to 4) with 0 being no detectable reaction and 4 being the most severe reaction. Erythema calculated from spectral analysis is expressed in oxy-hemoglobin values. Data are given as mean  $\pm 1$  standard deviation. The correlation coefficient of the two methods is  $R=0.979$ .



(a)



(b)

**Fig. 5** Evolution of skin inflammation can be monitored over time. (a) The difference of the apparent oxy-Hb value of the lesion compared to the surrounding uninvolved skin can be used as a measure of the erythema intensity of the lesion, and (b) the average lesion size as percentage change from day 1. Data are shown as mean  $\pm$  1 standard deviation for a total of 17 lesions of the five volunteers examined.

the vermillion. In parallel to the erythema map where all the inflammatory lesions can be clearly seen, the edema map shows only the ones that are at the stage of papules. Interestingly, these are the lesions that are most painful due to activation of the pain receptors by the local buildup of pressure.

The gray-level intensity of the erythema map has a linear relationship with the apparent concentration of oxy-Hb. This means that regions of interest (ROIs) can be drawn around each lesion and the apparent amount of oxy-Hb can be quantified and monitored over time. In this procedure, we used a circular ROI centered at the geometrical center of the lesion. The same ROI is used on the same lesion for all the images in the subsequent time points. The difference of the lesional erythema intensity from the erythema level of neighboring uninvolved skin can be recorded and plotted over time [Fig. 5(a)]. Another way of analysis is to threshold the erythema maps of the time sequence to the same limit and count the number of the non-zero-value pixels within the ROI of the lesion. This procedure gives an estimate of the lesion area. The percentage change in lesion area from baseline over time is shown in Fig. 5(b). Both the erythema intensity and the lesion size are relevant parameters that can be used to monitor the evolution of an acne inflammatory lesion over time.

### 3.3 Herpes Zoster

Spectral imaging was used to document the inflammatory reaction on a patient diagnosed with herpes zoster on the cheek and jaw area (Fig. 6). The oxy-Hb apparent concentration map provides better contrast than the conventional RGB image for erythema evaluation. Individual papules are easily detected as well as their agglomerations. Deoxy-Hb is slightly elevated in the inflamed area, though not to the levels of oxy-Hb, indicating the high demand for oxygen compared to surrounding tissue. Accumulation of extracellular fluid in the edematous areas can be demonstrated in the water apparent concentration map. These reactions are difficult or impossible to be identified in the visible image.

## 4 Discussion

In this paper, we demonstrated the applicability of spectral imaging to document skin inflammatory reactions. We provided examples of skin inflammation due to allergic contact dermatitis, inflammatory acne, and viral infection. In all cases, we demonstrated that using spectral imaging we can construct quantitative maps of apparent concentration of oxy-Hb and water corresponding to maps of erythema and edema. These maps not only give a visual aid of the distribution of erythema and edema, but they can also be used to calculate relevant parameters of disease progression, such as lesion count, lesion size, and erythema intensity.

The first model of skin inflammation we examined was rhus dermatitis. This condition is an allergic skin reaction caused by the *Rhus (toxicodendron)* genus of plants. Members of this genus are poison ivy, poison oak, and poison sumac. Plants in the *Rhus* genus produce an irritant pentadecylcatechol called urushiol in their stems, roots, canals, and skin of the fruits. When urushiol comes in contact with the skin, it causes an allergic reaction, commonly known as poison ivy rash.

Inflammatory acne is a common cutaneous disorder affecting males and females of all ages across the globe. It is a pleomorphic condition with multifactorial etiology. Its etiologic factors include hypercornification of the pilosebaceous duct, increased sebum production, and usually colonization by *Propionibacterium acnes*. Inflammatory acne manifests itself in the form of one or more lesions that typically take several days to weeks to resolve if left untreated. Acne lesions may have the form of macules (flat circumscribed areas of erythema that are not swollen), papules (raised lesions), and pustules (raised lesions that contain exudate). Therefore, edema may or may not be associated with an acne lesion.

Herpes zoster is a viral infection acquired at childhood. The virus lays dormant in the neurons until it is triggered in adulthood by yet unknown factors, though usually associated to stress. The manifestation of the disease is cutaneous inflammation that includes erythema, edema, and often severe pain.

In all cases of skin inflammation just mentioned, inflammatory cytokines and growth factors released from keratinocytes and other cells in the skin induce a chemical cascade that results in relaxation of the arteriolar smooth muscle, which eventually leads to vasodilation and increased vascular permeability. Vasodilation of capillaries in the papillary dermis leads to increased blood flow and increased local concen-

tration of blood. In this way, more oxygenated blood reaches the inflamed tissue. The strong blue-green absorption of hemoglobin gives the familiar red color (erythema) of the inflamed skin. In parallel, in some cases the increased vascular permeability leads to augmented interstitial fluid pressures. The onset of edema is the result of these osmotic pressures exceeding the lymphatic edema safety factors.<sup>22</sup>

Several papers have been published describing methods for measuring cutaneous erythema including colorimetric<sup>23–25</sup> or spectrophotometric methods.<sup>5–8,21</sup> In contrast to erythema, there are very few reports where spectroscopy was used to document the edema reaction.<sup>16</sup> All these methods are limited to the fact that the area measured is defined by the size of the probe. Furthermore, these methods require for the probe to come in contact with the skin, so that care must be taken to avoid cross-contamination of the measured skin areas.

In contrast, spectral imaging is a noncontact method in which the observed area is defined by the field of view of the objective and the resolution of the camera. Thus, it can be focused on a single lesion or extended to the whole face or whole body, as needed.

Spectral imaging in the visible and the NIR range has been used in the study of blood oxygenation level as an indicator of tissue survival in burns<sup>26</sup> or grafts.<sup>27</sup> It has also been proposed for the diagnosis of hemorrhagic shock.<sup>28</sup> We recently reported the use of spectral imaging to document cutaneous edema following histamine iontophoresis.<sup>15</sup>

In this paper, we demonstrated *in vivo* functional imaging of cutaneous inflammatory reactions using characteristic absorption bands of water and hemoglobin. Apparent concentration maps of oxy-Hb and water were constructed that represent quantitative visualizations of the intensity and extent of erythema and edema correspondingly. These maps can be used to extract relevant information for the assessment of the severity or to monitor the evolution of a cutaneous inflammatory reaction. The portability of the method presented here enables it to easily be adapted in a clinical or dermatology practice setting. The fact that erythema and edema are the primary clinical expressions of tissue inflammation indicates that the present method may be exploited in a wide range of medical applications following the appropriate modifications, for example, used with a catheter to document tissue inflammation during surgery.

### Acknowledgments

The authors would like to acknowledge the contributions of Dr. Kays Keidbey of KGL Inc. and Laura Magee of Johnson & Johnson CPPW for the poison ivy study and of Jeannette Chantalat of Johnson & Johnson CPPW for her contribution to the acne study. The authors would like to acknowledge Prof. Costas Balas of FORTH-Photonics for the development of the hyperspectral camera.

### References

1. A. E. Taylor, "Capillary fluid filtration. Starling forces and lymph flow," *Circ. Res.* **49**, 557–575 (1981).
2. G. Zonios, J. Bykowski, and N. Kollias, "Skin melanin, hemoglobin, and light scattering properties can be quantitatively assessed *in vivo* using diffuse reflectance spectroscopy," *J. Invest. Dermatol.* **117**, 1452–1457 (2001).
3. W. Verkruysse, R. Zhang, B. Choi, G. Lucassen, L. O. Svaasand, and J. S. Nelson, "A library based fitting method for visual reflectance spectroscopy of human skin," *Phys. Med. Biol.* **50**, 57–70 (2005).
4. L. O. Svaasand, L. T. Norvang, E. J. Fiskerstrand, E. K. S. Stopps, M. W. Berns, and J. S. Nelson, "Tissue parameters determining the visual appearance of normal skin and port-wine stains," *Lasers Med. Sci.* **10**, 55–65 (1995).
5. N. Kollias, R. Gillies, J. A. Muccini, R. K. Ueyama, S. B. Phillips, and L. A. Drake, "A single parameter, oxygenated hemoglobin, can be used to quantify experimental irritant-induced inflammation," *J. Invest. Dermatol.* **104**, 421–424 (1995).
6. N. Kollias and A. H. Baqer, "Quantitative assessment of UV-induced pigmentation and erythema," *Photodermatol.* **5**, 53–60 (1988).
7. R. R. Anderson and J. A. Parrish, "The optics of human skin," *J. Invest. Dermatol.* **77**, 13–19 (1981).
8. P. H. Andersen and P. Bjerring, "Spectral reflectance of human skin *in vivo*," *Photodermatol. Photoimmunol. Photomed.* **7**, 5–12 (1990).
9. G. N. Stamatas and N. Kollias, "Blood stasis contributions to the perception of skin pigmentation," *J. Biomed. Opt.* **9**, 315–322 (2004).
10. R. Marchesini, S. Tomatis, C. Bartoli, A. Bono, C. Clemente, C. Cupeta, I. Del Prato, E. Pignoli, A. E. Sichirollo, and N. Cascinelli, "In vivo spectrophotometric evaluation of neoplastic and non-neoplastic skin pigmented lesions. III. CCD camera-based reflectance imaging," *Photochem. Photobiol.* **62**, 151–154 (1995).
11. D. L. Farkas and D. Becker, "Applications of spectral imaging: detection and analysis of human melanoma and its precursors," *Pigment Cell Res.* **14**, 2–8 (2001).
12. K. J. Zuzak, M. D. Schaeberle, E. N. Lewis, and I. W. Levin, "Visible reflectance hyperspectral imaging: characterization of a noninvasive, *in vivo* system for determining tissue perfusion," *Anal. Chem.* **74**, 2021–2028 (2002).
13. V. P. Zharov, S. Ferguson, J. F. Eidt, P. C. Howard, L. M. Fink, and M. W. Wamer, "Infrared imaging of subcutaneous veins," *Lasers Surg. Med.* **34**, 56–61 (2004).
14. G. N. Stamatas, C. Balas, and N. Kollias, "Hyperspectral image acquisition and analysis of skin," *Proc. SPIE* **4959**, 77–82 (2003).
15. G. N. Stamatas, M. Southall, and N. Kollias, "In vivo monitoring of cutaneous edema using spectral imaging in the visible and near infrared," *J. Invest. Dermatol.* **126**, 1753–1760 (2006).
16. S. Shibata, H. Ohdan, T. Noriyuki, S. Yoshioka, T. Asahara, and K. Dohi, "Novel assessment of acute lung injury by *in vivo* near-infrared spectroscopy," *Am. J. Respir. Crit. Care Med.* **160**, 317–323 (1999).
17. U. Hampel, E. Schleicher, E. G. Wustenberg, and K. B. Huttenbrink, "Optical measurement of nasal swellings," *IEEE Trans. Biomed. Eng.* **51**, 1673–1679 (2004).
18. K. H. Kaidbey and A. M. Kligman, "Assay of topical corticosteroids. Efficacy of suppression of experimental Rhus dermatitis in humans," *Arch. Dermatol.* **112**, 808–813 (1976).
19. H. Xie, N. Hicks, G. R. Keller, H. Huang, and V. Kreinovich, "An IDL/ENVI implementation of the FFT-based algorithm for automatic image registration," *Comput. Geosci.* **29**, 1045–1055 (2003).
20. G. N. Stamatas, B. Z. Zmudzka, N. Kollias, and J. Z. Beer, "Non-invasive measurements of skin pigmentation *in situ*," *Pigment Cell Res.* **17**, 618–626 (2004).
21. J. K. Wagner, C. Jovel, H. L. Norton, E. J. Parra, and M. D. Shriver, "Comparing quantitative measures of erythema, pigmentation and skin response using reflectometry," *Pigment Cell Res.* **15**, 379–384 (2002).
22. A. E. Taylor, "The lymphatic edema safety factor: the role of edema dependent lymphatic factors (EDLF)," *Lymphology* **23**, 111–123 (1990).
23. J. Serup and T. Agner, "Colorimetric quantification of erythema—a comparison of two colorimeters (Lange Micro Color and Minolta Chroma Meter CR-200) with a clinical scoring scheme and laser-Doppler flowmetry," *Clin. Exp. Dermatol.* **15**, 267–272 (1990).
24. A. Fullerton, T. Fischer, A. Lahti, K. P. Wilhelm, H. Takiwaki, and J. Serup, "Guidelines for measurement of skin colour and erythema. A report from the Standardization Group of the European Society of Contact Dermatitis," *Contact Dermatitis* **35**, 1–10 (1996).
25. I. L. Weatherall and B. D. Coombs, "Skin color measurements in terms of CIELAB color space values," *J. Invest. Dermatol.* **99**, 468–473 (1992).
26. M. G. Sowa, L. Leonardi, J. R. Payette, J. S. Fish, and H. H. Mantsch, "Near infrared spectroscopic assessment of hemodynamic changes in the early post-burn period," *Burns* **27**, 241–249 (2001).

27. J. R. Payette, M. G. Sowa, S. L. Germscheid, M. F. Stranc, B. Abdulrauf, and H. H. Mantsch, "Noninvasive diagnostics: predicting flap viability with near-IR spectroscopy and imaging," *Am. Clin. Lab.* **18**, 4–6 (1999).
28. L. C. Cancio, A. I. Batchinsky, J. R. Mansfield, S. Panasyuk, K. Hetz, D. Martini, B. S. Jordan, B. Tracey, and J. E. Freeman, "Hyperspectral imaging: a new approach to the diagnosis of hemorrhagic shock," *J. Trauma* **60**, 1087–1095 (2006).